

Classification: Biological Science, Biochemistry

A novel heme degradation pathway in a blood-sucking insect

Gabriela O. Paiva-Silva^{**†}, Christine Cruz-Oliveira^{**†}, Ernesto S. Nakayasu^{†,‡}, Clarissa M. Maya-Monteiro[§], Boris C. Dunkov[¶], Hatisaburo Masuda^{*}, Igor C. Almeida^{†,‡,¶} **||** & Pedro L. Oliveira^{*,||}

*Instituto de Bioquímica Médica, Programa de Biologia Molecular e Biotecnologia, Universidade Federal do Rio de Janeiro, Rio de Janeiro, 21941-590, Brazil

†Department of Biological Sciences, University of Texas at El Paso, El Paso, TX 79968-0519, USA

‡Departamento de Parasitologia, Universidade de Sao Paulo, Sao Paulo, SP 05508-900, Brazil

§Departamento de Fisiologia e Farmacodinâmica, Instituto Oswaldo Cruz, Rio de Janeiro, RJ, 21045-900, Brazil

¶Department of Biochemistry and Molecular Biophysics; Center for Insect Science, University of Arizona, Tucson, AZ 85721, USA

**G.O.P.S. and C.C.O. contribute equally to the work.

|| To whom correspondence should be addressed.

Corresponding authors:

Pedro L. Oliveira, Instituto de Bioquímica Médica, Programa de Biologia Molecular e Biotecnologia, Universidade Federal do Rio de Janeiro, CCS, sala 5 Bloco D subsolo, Ilha do Fundão, Rio de Janeiro, 21941-590, Brazil, tel:55(21)25626751, fax:55(21)22905436 (pedro@bioqmed.ufrj.br);

Igor C. Almeida, Department of Biological Sciences, University of Texas at El Paso, 500 W. University Ave., El Paso, TX 79968-0519, USA, tel: (915)7476086, fax: (915)747-5808, (icalmeida@utep.edu).

Abstract

Hematophagous insects are vectors of diseases that affect hundreds of millions of people worldwide. A common physiological event in the life of these insects is the hydrolysis of host hemoglobin in the digestive tract leading to a massive release of heme, a known pro-oxidant molecule. Diverse organisms, from bacteria to plants, express the enzyme heme oxygenase (HO), which catalyzes the oxidative degradation of heme to biliverdin IX, CO, and iron. Here we show that the kissing bug *Rhodnius prolixus*, a vector of Chagas' disease, has a unique heme degradation pathway wherein heme is first modified by addition of two cysteinylglycine residues before cleavage of the porphyrin ring, followed by trimming of the dipeptides. Furthermore, in contrast to most known heme oxygenases, which generate biliverdin IX α , in this insect the end product of heme detoxification is a dicysteinyl-biliverdin IX γ . Based on these results, we propose a new heme metabolizing pathway that includes the identified intermediates produced during modifications and cleavage of the heme porphyrin ring.

Introduction

Heme is a ubiquitous molecule that is involved in many essential biological processes, including oxygen transport, respiration, photosynthesis, drug detoxification and signal transduction (1). However, free heme is a potent pro-oxidant, leading to the formation of reactive oxygen species that can damage a variety of biological molecules (2). Furthermore, heme can associate with phospholipid membranes, altering bilayer structure and, thus, causing cell disruption (3,4). For this reason, the cells strictly regulate heme homeostasis. An important component of this control is heme oxygenase (HO), an enzyme that is expressed by organisms as diverse as bacteria and plants (5-7). Heme degradation by HO proceeds by a multistep mechanism that involves rapid hydroxylation at one of the *meso*-carbon of the porphyrin ring, the α -*meso*-carbon in most of the organisms, oxygen-dependent elimination of the hydroxylated *meso*-carbon as CO-producing verdoheme, and oxidative cleavage of verdoheme to biliverdin IX in a reaction dependent on reducing equivalents and O₂, with concomitant release of Fe²⁺ (6-9). This heme degradation pathway has been extensively studied in the last decade, not only for its role in heme detoxification and iron recycling (2), but also because the cleavage products of the porphyrin ring, biliverdin and CO, play important physiological roles (10). In mammals, CO, a gaseous messenger, has anti-inflammatory (11) and anti-apoptotic (12) effects, and it is clear that biliverdin and its reduced product bilirubin may function as important antioxidants (13-16). Moreover, in algae and higher plants biliverdin is a precursor for the synthesis of essential chromophores (17,18).

Biliverdins and their derivatives, associated with different proteins, are found in the hemolymph and integument of insects of different orders (19), providing camouflage, especially for larvae feeding on plants. However, in hematophagous insects, heme

degradation has been overlooked, in spite of the fact that these insects undoubtedly have to deal with one of the highest dietary heme concentrations in nature. These animals face an intense oxidative stress condition upon degradation of host hemoglobin during digestion. Thus, in the course of evolution, these animals have developed an array of strategies to counteract heme cytotoxicity, in order to adapt successfully to blood feeding (20-23).

Here we have investigated heme degradation in the blood-sucking bug *Rhodnius prolixus*, the vector of *Trypanosoma cruzi*, the etiologic agent of Chagas' disease or American trypanosomiasis. We show that in contrast to all other organisms studied to present, heme breakdown follows a complex pathway with four distinct intermediates and results in dicysteinyl-biliverdin IX γ as the end product.

Results

Biliverdin production in *Rhodnius prolixus*

The heart of the blood-sucking bug *Rhodnius prolixus* is green in color due to the accumulation of pigment in the pericardial cells (Fig. 1A). This pigment, also observed in midgut cells (Fig. 1B), was assumed to be identical to biliverdin (24). While the midgut would have been an obvious choice to study heme degradation in a blood-feeding animal, we decided to perform most of the experiments with the insect heart. This was done because the presence of large amounts of heme in the gut presented experimental difficulties, especially concerning the HPLC separation of some heme metabolites that are described below. To investigate whether the green pigment was produced from heme degradation, we injected female insects with ^{14}C -heme bound to RHBP, a *R. prolixus* heme-binding protein that is able to transport heme to many tissues including the heart (25). Reverse-phase HPLC analysis of heart homogenates (Fig. 1C) revealed a single major radioactive peak that shows a light-absorption spectrum typical of biliverdin, with λ_{max} at 360 nm and 689 nm (Fig. 1D). However, this *R. prolixus* biliverdin (RpBV) was eluted with a more hydrophilic retention time than biliverdin IX α (BV IX α), the canonical product of heme degradation catalyzed by heme oxygenase (HO) (Fig. 1C). This suggested the existence of structural differences between RpBV and BV IX α . The same result was also obtained from the analysis of midgut homogenates (data not shown). Furthermore, injecting heme into the hemocoel induced accumulation of RpBV in the pericardial cells *in vivo*, a process that was inhibited by co-injecting Sn-protoporphyrin IX (SnPP IX), a classical inhibitor of HO (Fig. 1E).

Electrospray ionization mass-spectrometry (ESI-MS) analysis revealed that the purified RpBV has a molecular mass of 824.2 Da ($[\text{RpBV} + \text{H}]^+$ at m/z 825.2, and $[\text{RpBV} + 2\text{H}]^{2+}$ at m/z 413.1), higher than that of biliverdin IX α ($[\text{BV IX}\alpha + \text{H}]^+$ at m/z 583.2) (Fig. 2A).

Analysis of sequential fragmentation by tandem ESI-MS indicated that RpBV produced a major ion species of m/z 704, by the loss of a residue of 121 Da (Fig. 2B). A RpBV daughter-ion species with the same molecular mass as BV IX α (m/z 583.2) was generated by fragmentation of the m/z 704 ion species, again by removal of 121 Da (Fig. 2B). These results demonstrated that RpBV comprises BV coupled to two residues of 121 Da. Fragmentation of both the RpBV ion species of m/z 122 and a cysteine standard produced almost identical daughter ion species (Fig. 2C), suggesting that the 121 Da residues coupled to BV were most likely cysteine residues.

Most of the described heme oxygenases hydroxylate heme at the α -*meso*-carbon position, producing exclusively BV IX α (6-9). Recently, two exceptions were reported: the *Pseudomonas aeruginosa* HO, capable of degrading heme to both δ and β isomers of BV (26), and the recombinant *Drosophila melanogaster* HO, which produced simultaneously δ , β , and α BV isomers in vitro (27). Since it is well established that some insects produce BV IX γ (19), we investigated the possibility that RpBV is also the γ isomer. Fragmentation of BV IX γ and the RpBV ion species at m/z 583 produced identical daughter ion species (Fig. 2D). This fragmentation pattern was clearly distinct from that obtained by fragmentation of BV IX α (Fig. 2D). In support of this, the light-absorption spectrum of RpBV indeed closely resembled that of BV IX γ (Fig. 1D). These results indicate the existence in *R. prolixus* of heme-degrading activity with distinct regiospecificity, capable of cleaving the porphyrin ring at the γ -*meso*-position.

Taken together, our results clearly demonstrate that the product of the heme degradation pathway in *R. prolixus* is BV IX γ conjugated to two cysteine residues. In order to investigate how the two cysteine residues were attached to BV IX γ , we produced chemical modifications of the potentially free amino, carboxyl, and thiol groups of the RpBV cysteine residues by

acetylation, methylation, and alkylation reactions, respectively (Fig. 5, as supporting information on the PNAS web site). As expected, BV IX γ (m/z 583.3) was not modified after acetylation, since it has no free amino groups (Fig. 5A). In contrast, the acetylation product of RpBV was an ion species at m/z 909.5 (Fig. 5B), which corresponds to the addition of one acetyl group (42 Da) to each free amino group of the two cysteine residues, demonstrating that these amino groups are free, thus not being involved in the binding of cysteine to biliverdin. Methylation of one and two carboxyl groups of the propionate side chains of BV IX γ produced the ion species at m/z 597.4 and m/z 611.4, respectively (Fig. 5C). Methylation of RpBV produced ion species containing three (m/z 867.5) or four (m/z 881.5) modifications, indicating that in RpBV, a total of four carboxyl groups are available for methylation (two from the BV propionate residues and two from the cysteine residues) (Fig. 5D). These results indicate that neither the cysteine carboxyl groups nor the carboxyl groups of BV propionyl side chains are involved in the attachment of the two cysteine residues to BV. Alkylation reaction that should have modified free SH groups did not affect RpBV (Fig. 5E), demonstrating that the cysteine thiol groups were involved in the binding of the amino acids to BV.

Our results clearly indicated that the cysteine residues were attached to the vinyl side chains of BV IX γ by thioether bonds (Fig. 5F). This is similar to the attachment of heme to the cysteine residues of c-type cytochromes (28), and to the binding of biliverdin to the *Agrobacterium* phytochromes Agp 1 (29).

Identification of heme degradation pathway intermediates

In order to determine whether the addition of cysteine occurred before or after the cleavage of the porphyrin ring, female insects were co-injected with heme and Sn-protoporphyrin IX. Homogenates of insect hearts were then analyzed by HPLC and two peaks showed

substantial increase, when compared to controls (Fig. 3A). Interestingly, the light-absorption spectra of these peaks displayed typical heme Soret bands (Fig. 3A, inset). However, as observed for RpBV, these compounds were more hydrophilic than heme, suggesting that they could be modified heme intermediates of the heme degradation pathway produced before the oxidative cleavage of the porphyrin ring. To test this hypothesis, purified intermediates were analyzed by tandem ESI-MS for structure determination. The most hydrophilic compound, intermediate 2 (Int 2), showed a major singly-charged ion species at m/z 972.2, whereas intermediate 1 (Int 1), eluting closer to heme, showed a major singly-charged ion species at m/z 794.2 (Fig. 3B). Sequential fragmentation of both intermediates by tandem ESI-MS/MS produced an ion species at m/z 776 (Fig. 6A and B, as supporting information on the PNAS web site), which after further fragmentation generated an ion species at m/z 616 (Fig. 3C, upper spectrum). This species, in turn, generated daughter species identical to an authentic heme (Fig. 3C and D), confirming that these intermediates were modified heme products. Further evidence that intermediates 1 and 2 are part of the RpBV production pathway was obtained by injecting insects with heme and ^{35}S -cysteine, which resulted in incorporation of label in the peaks of both intermediates (data not shown). However, the molecular masses of intermediates 1 and 2 were not consistent with the simple addition of one and two cysteine residues to heme. Instead, they are produced by attachment of one and two identical molecules of 178 Da, respectively. These molecules were shown by tandem ESI-MS to be the dipeptide cysteinylglycine (Fig. 6C and D), a compound normally produced in mammals by intracellular metabolism of glutathione (30). Thus, we conclude that the intermediates 1 and 2 are monocysteinylglycine-heme and dicysteinylglycine-heme, respectively. The proposed assignments for the parent molecular-ion species for each intermediate and the relatively more abundant daughter-ion species are shown in Figure 6C and D.

Additionally, reverse-phase HPLC analysis of heart homogenates from insects injected with mesoheme (vinyls replaced by ethyls) did not reveal any compound with elution volume and/or light-absorption spectrum typical of underivatized mesobiliverdin IX (Fig. 7, as supporting information on the PNAS web site). This result strongly suggests that addition of the cysteinylglycine residues to heme vinyl groups are needed to allow efficient oxidation and cleavage of the porphyrin ring.

These findings were unexpected since no such alterations of heme structure have been described before. Therefore, we decided to identify the intermediates downstream from intermediate 2 by injecting insects with heme and analyzing heart homogenates by LC-MS. By this procedure, we detected two intermediates, one of m/z 939.3 and another of m/z 882.3 (Fig. 8, as supporting information on the PNAS web site). These molecules corresponded respectively to biliverdin coupled with two cysteinylglycine residues (intermediate 3, Int 3) and biliverdin bound to one cysteine and one cysteinylglycine (intermediate 4, Int 4) (Fig. 9C and D, as supporting information on the PNAS web site). Fragmentation of these molecules produced common daughter-ion species (Fig. 8A and B), some identical to those produced by fragmentation of RpBV (m/z 686 and m/z 704) (Fig. 2B), thus confirming that they are precursors of RpBV.

Based on these findings we propose that in *R. prolixus* heme catabolism involves three distinct steps: i) modification of heme by two consecutive additions of cysteinylglycine dipeptides or glutathione, in the latter case followed by removal of the glutamic residues; ii) oxidative cleavage of the porphyrin ring of dicysteinylglycine-heme to dicysteinylglycine-BV IX γ ; iii) hydrolysis of the cysteine-glycine peptide bonds by a dipeptidase, releasing the end product RpBV, a dicysteinyl-BV IX γ . The proposed heme degradation pathway is represented schematically in Figure 4.

Discussion

In all cases reported until now heme breakdown is accomplished by HO, a single enzyme that produces BV IX. Here, for the first time, we describe a pathway where heme is chemically modified prior to oxidative cleavage of the porphyrin ring, leading to accumulation of a dicysteinyl-biliverdin IX γ as the main end product.

The first modified form of heme we found was a cysteinylglycine-heme. The most plausible explanation for the production of this compound would involve glutathione as the donor of the cysteinylglycine dipeptide. When the complete heme modification pathway is considered, it is remarkable that exactly the same group of reactions, involving conjugation and processing of glutathione, operates during the synthesis of cysteinyl-leukotrienes from leukotriene A4 in mammalian cells (31). In smooth muscle cells, the addition of glutathione to leukotriene A4 is performed by a microsomal glutathione S-transferase, member of a class of enzymes known for their involvement in the detoxification of endogenous or xenobiotic compounds in many organisms (31). Cysteinylglycine-leukotrienes are then trimmed by the action of proteases generating cysteinyl-leukotrienes.

However, since we did not find a glutathione-heme intermediate, we can not exclude that cysteinylglycine itself may be the substrate for the initial heme modification. Alternatively, one could also speculate that a glutathione molecule may be first added to heme by a specific lyase activity and then, glutamic acid is removed by a γ -glutamyl-transpeptidase (30). Lyase activities are involved in the attachment of heme to apocytochrome C (32) and of a biliverdin-derived chromophore, phycocyanobilin, to the apophycocyanin, in the cyanobacterium *Synechococcus* sp. (33).

The biochemical and physiological significance of the addition of hydrophilic residues to heme molecules is unclear. Perhaps this could be a way to achieve the excretion of large

amounts of biliverdin, a non-hydrophilic molecule, produced after blood digestion. Similarly, in mammals bilirubin is excreted only after conjugation to glucuronic acid. Failure in this process results in the massive accumulation of bilirubin can lead to neurotoxic damage as observed in Crigler-Najjar Syndrome (34-37). Therefore, these adaptations could represent a case of convergent evolution, resulting in the effective prevention of membrane damage and cytotoxicity by the accumulation of the hydrophobic heme degradation products.

The production of a BV IX γ isomer indicates that *R. prolixus* expresses a HO enzyme capable of cleaving the porphyrin ring at the γ position. Recent elegant works have shown that the position of heme hydroxylation is determined by ionic interactions between heme and the HO enzyme (38-42). In addition, mutations of some specific HO charged amino acid residues lining the active site cavity that interact with heme propionic acid groups cause alterations of heme oxidation regiospecificity (42). In the case of RpBV production, we could hypothesize that the presence of charged cysteine carboxyl groups in the unusual substrate, intermediate 2, may establish specific ionic interactions between this modified heme and HO, determining a γ -specific cleavage. Besides, it is feasible to speculate that *R. prolixus* HO may present particular differences in its active site conformation that allow it to accommodate this modified heme. Thus, the *R. prolixus* system described here gives new insights and could provide a unique model to better understand lesser-known aspects of the chemistry and biology of heme degradation.

Finally, production of both oxygen and nitrogen radicals as a pathogen-killing mechanism is a hallmark of innate immunity. Therefore, redox balance – the equilibrium between oxidative challenge and protective detoxification mechanisms – is a critical factor in the interaction between microorganisms that live in the gut lumen and the epithelial cells of the midgut, as shown for both mosquito-transmitted pathogens (42), and for bacterial intestinal flora of *Drosophila* (43). In the latter report, it was shown that silencing of an extracellular immune-

related catalase in the midgut of *Drosophila* causes high mortality in flies after ingestion of live or even dead bacteria due to an intense oxidative damage to midgut cells.

HO is well known as one of the most prominent proteins taking part in the stress response of eukaryotic cells (44). Therefore, the existence of the unique pathways described here suggests that stress-response in hematophagous animals may differ significantly from that found in other organisms.

Multiple lines of evidence clearly indicate that hematophagy has appeared independently several times during the evolution of arthropods (45), *i.e.*, different groups of present day hematophagous animals derive from a non-hematophagous ancestor. Thus, in the course of their evolution, several different protective mechanisms have evolved, allowing these organisms to be successfully adapted to blood feeding. In conclusion, our results demonstrate the existence of several activities involved in heme detoxification, employed in a strategy that could be possibly shared by other hematophagous insects. Characterization of such heme metabolizing systems and their role as a defense mechanism against heme toxicity could help to understand the molecular basis of the adaptation to a blood-feeding lifestyle. Moreover, it could also establish a new and important component of the interaction between pathogens and insect hosts. In addition, such studies could lead to the discovery of interesting targets for drug design and vector control strategies, allowing the development of highly specific insecticides and/or manipulation of the vector's ability to transmit parasites.

Materials and Methods

Chemicals and preparation of biliverdin IX γ . Hemin (Fe(III) protoporphyrin IX chloride), Fe(III) mesoporphyrin IX chloride, Sn(IV)-protoporphyrin IX, and biliverdin IX α were purchased from Frontier Scientific (Logan UT). Biliverdin IX γ , the chromophore of the *Manduca sexta* biliprotein insecticyanin was extracted from larval hemolymph (46). Hemolymph collected in cold 20 mM Tris HCl, 100 mM NaCl buffer, pH 8.0, saturated with phenylthiourea was centrifuged at 1,000 x g to remove hemocytes and any precipitates. After acidification (by adding 0.2 ml 5 N HCl and 0.2 ml glacial acetic acid to each ml of hemolymph) biliverdin IX γ was extracted into an equal volume of chloroform. The chloroform layer was washed three times with water and evaporated under a stream of nitrogen. To remove remaining contaminants, biliverdin IX γ was dissolved quickly in chloroform, transferred to a fresh tube, and dried again. The biliverdin IX γ residue was stored under nitrogen atmosphere, protected from light at -20°C . Hemin, Fe(III) mesoporphyrin IX chloride, Sn-protoporphyrin IX and biliverdin stock solutions were freshly prepared in 0.1 mM NaOH or DMSO.

Insects, treatments, and pigment extraction. *Rhodnius prolixus* were maintained at 28°C and 70 % relative humidity. Mated female insects, fed on rabbit blood at 3-week intervals, were used in all experiments. (^{14}C -heme) Rhodnius heme-binding protein (RHBP) was obtained as previously described (47). Injections were performed as described (25). Dissected insect hearts were homogenized in PBS, pH 7.4 and centrifuged for 5 min at 12,000 x g. Supernatants were kept protected from light, and stored at -20°C until use.

HPLC fractionation. HPLC on a Shimadzu CLC-ODS C18 column (15 mm x 22 cm) was performed using a Shimadzu LC-10AT device (Tokyo, Japan) equipped with a diode array

detector (SPD-M10A). Chromatography analysis was performed using 5 % acetonitrile with 0.05 % trifluoroacetic acid (TFA) as solvent, at a flow rate of 0.4 ml/min. Before injection, samples were diluted 2X in 5 % acetonitrile with 0.05 % TFA and centrifuged for 15 min at 12,000 x *g*. Ten minutes after injection of the sample, a 40-min linear acetonitrile gradient (5–80 %) was applied, and the final concentration was maintained for 20 min. For identification and characterization of intermediates, heart homogenates were analyzed by nano-HPLC (Ultimate, LC Packings, Dionex, Sunnyvale, CA) using a laboratory-made reverse phase capillary column, assembled in a 10-cm fused silica capillary (75 µm I.D. x 360 µm O.D., Polymicro Technologies Inc., Phoenix, AZ) with a C18 resin (10-15 µm, 300Å, Vydac, Hesperia, CA). Chromatography conditions were as described above except that TFA was replaced by formic acid and the flow rate was 0.2 µl/min.

Absorption spectroscopy. Light absorption spectra were obtained from biliverdin isomers and purified RpBV dissolved in methanol:HCl (95:5 v/v). Spectra of heme, mesoheme and modified heme intermediates were recorded during the chromatography by the HPLC diode array detector.

Electrospray ionization mass spectrometry (ESI-MS). Mass spectra were obtained in the positive ion mode using a Finnigan LCQ-Duo ion trap mass spectrometer (Thermo Electron Co., San Jose, CA). Heart homogenates and biliverdin IX stock solutions were prepared in 50 % acetonitrile, 0.1 % formic acid. Heme stock solutions were prepared in 100 % DMSO and diluted in 50 % methanol immediately before use. Samples were introduced into the electrospray source by injection through a 50-µm internal diameter fused silica capillary at a 5 µl/min flow rate. ESI source and capillary voltages were set at 36-46 V and 4.5 kV, respectively; the capillary temperature was 250°C. Spectra were acquired at 3 s/scan. Collision-induced fragmentation (tandem ESI-MS) of parent ions was carried out using a

relative collision energy of 30-50 % (1.5-2.5 eV). For the analysis of intermediates, all fractions eluted from the nano-HPLC column were subjected to tandem ESI-MS and selective ion-monitoring (SIM) (for ions at m/z 794.2, 825.3, 882.3, 939.3, and 972.2), and the most abundant ion species of each fraction was subjected to tandem ESI-MS. ESI capillary voltage was set at 1.9 kV, and the temperature at 180°C. Source-induced dissociation (SID) (cone fragmentation) was achieved by applying a cone fragmentation voltage of 10 V.

N-acetylation of free amino groups of RpBV. Purified biliverdin IX γ and RpBV were resuspended in pre-cooled 100 μ L 1M NH₄OH. After addition of 2.5 μ l acetic anhydride, samples were incubated for 10 min at 4 °C. This step was repeated 2 times. After incubation at 25 °C for 30 min, samples were dried under vacuum and resuspended in 50 % acetonitrile, 0.1 % formic acid for ESI-MS analysis.

Methylation of carboxyl groups of BV IX γ and RpBV. Purified biliverdin IX γ and RpBV were resuspended in 100 μ l NH₄OH. After addition of 100 μ l 100% methanol, samples were incubated for 1 h at 37 °C. Samples were dried under vacuum and washed two times with 100 μ l 100% methanol. The precipitates were resuspended in 100 μ l 100% methanol and incubated for 1 h at 75 °C. After addition of tert-butanol (20 μ l) samples were dried under vacuum and resuspended in 50 % acetonitrile, 0.1 % formic acid for ESI-MS analysis.

Alkylation of RpBV free SH groups. Purified Biliverdin IX γ and RpBV were resuspended in 50 μ L 0.6 M Tris HCl, 6 M guanidine hydrochloride. After addition of 50 μ l 4 mM DTT, samples were incubated for 45 min at 45 °C under N₂ atmosphere. 0.5 M iodoacetamide (50 μ l) were added to the reaction and samples were incubated for 10 min at 45 °C under N₂ atmosphere. Reaction was stopped by addition of 150 μ l 0.046% TFA. Samples were dried under vacuum and resuspended in 50 % acetonitrile, 0.1 % formic acid for ESI-MS analysis.

Acknowledgments:

We thank J.S. Lima Jr and L.M. Rodrigues, H.S.L. Coelho, L.S.C. Gomes, S.J. Tadeu and S.R. de Cassia for valuable technical assistance; N.A. Assunção for making the capillary columns and M. Sorenson for critical reading of the paper. This work was supported by grants from CNPq, CAPES, FAPERJ, PRONEX, Howard Hughes Medical Institute (HHMI). C.M.M. was supported by a fellowship from Fundação do Instituto Oswaldo Cruz. I.C.A. was supported by FAPESP (grant # 98/10495-5) and BBRC/Biology/UTEP (NIH grant # 5G12RR008124); B.C.D. was supported by National Institutes of Health grant (GM58918).

References

- 1- Ponka, P. (1999) *Am. J. Med. Sci.* **318**, 241-256.
- 2- Ryter, S. W. & Tyrrel, R. M. (2000) *Free Radical Biol.Med.* **28**, 289-309.
- 3- Chou, A. C. & Fitch, C. D. (1980) *J. Clin. Invest.* **66**, 856-858.
- 4- Schmitt, T. H., Frezzati Jr., W. A. & Schreier, S. (1993) *Arch.Biochem. Biophys.* **307**, 96-103.
- 5- Tenhunen R., Marver H. S., Schmid R. D. (1969) *J. Biol. Chem.* **244**, 6388–6394.
- 6- Ortiz de Montellano, P. R. & Wilks, A. (2000) *Adv. Inorg. Chem.* **51**, 359-407.
- 7- Ortiz de Montellano, P. R. (2000) *Curr. Opin. Chem. Biol.* **4**, 221–227.
- 8- Yoshida, T. & Taiko Migita, C. (2000) *J. Inorg. Biochem.* **82**, 33–41.
- 9- Wilks, A. (2002) *Antioxid. Redox Signal.* **4**, 603-614.
- 10- Maines, M. D. (1997) *Annu. Rev. Pharmacol. Toxicol.* **37**, 517-554.
- 11- Otterbein L. E., Bach, F. H., Alan , J., Tao Lu, H., Wysk, M., Davis, R. J., Flavell, R. A. & Choi, A. M. (2000) *Nat. Med.* **6**, 422-428.
- 12- Brouard S., Berberat, P. O., Tobiasch, E, Seldon, M. P., Bach, F. H. & Soares M. P. (2002) *J. Biol. Chem.* **277**, 17950-17961.
- 13- Stocker, R., Yamomoto, Y., McDonagh, A. F., Glazer, A. N. & Ames, B. N. (1987) *Science* **235**, 1043-1046.
- 14- Dore, S. & Snyder, S. H. (1999). *Ann. N Y Acad. Sci.* **890**, 167-172.
- 15- Sedlak, T. W. & Snyder, S. H. (2004) *Pediatrics* **113**, 1776-1782.
- 16- Stocker, R. (2004) *Antioxid. Redox Signal.* **5**, 841-849.
- 17- Terry, M. J., Wahleithner, J. A. & Lagarias, J. C. (1993) *Arch. Biochem. Biophys.* **306**, 1-15.
- 18- Smith, H. (2000) *Nature* **407**, 585-591.

- 19- Kayser, H. (1985) in *Comprehensive Insect Physiology, Biochemistry and Pharmacology*, eds. Kerkut, G.A. & Gilbert, L.I. (Pergamon Press, Oxford), vol 10, pp. 367-415.
- 20- Dansa-Petretski, M., Ribeiro, J. M. C., Atella, G. C., Masuda, H. & Oliveira, P. L. (1995) *J. Biol.Chem.* **270**, 10893-10896.
- 21- Oliveira, M. F., Silva, J. R., Dansa-Petretski, M., de Souza, W., Lins, U., Braga, C. M., Masuda, H., & Oliveira, P. L. (1999) *Nature* **400**, 517.
- 22- Oliveira, M. F., Timm, B. L., Machado, E. A., Miranda, K., Attias, M., Silva, J. R., Dansa-Petretski, M., de Oliveira, M. A., de Souza, W., Pinhal, N. M., Sousa, J. J., Vugman, N. V. & Oliveira P. L. (2002) *FEBS letter* **512**, 139-144.
- 23- Pascoa, V., Oliveira, P. L., Dansa-Petretski, M., Silva, J. R., Alvarenga, P. H., Jacobs-Lorena, M. & Lemos, F. J. (2002) *Insect Biochem. Mol.Biol.* **32**, 517-523.
- 24- Wigglesworth, V. B. (1943) *Proc. Roy. Soc. Lond. B* **131**, 313-339.
- 25- Machado E. A., Oliveira, P. L., Moreira, M. F., de Souza, W. & Masuda, H. (1998). *Arch. Insect Biochem. Physiol.* **39**,133-143. Holden, H. M., Rupnievski, W. R., Law, J. H. & Rayment, I. (1987) *EMBO J.* **6**,1565-1570.
- 26- Ratliff, M., Zhu, R., Wilks, A. & Stojiljkovic, I. (2001) *J. Bacteriol.* **183**, 6394-6403.
- 27- Zhang, X., Sato, M., Sasahara, M. Migita, C. & Yoshida, T. (2004) *Eur. J. Biochem.* **271**, 1713-1724.
- 28- Basile, G., Di Bello, C.& Taniuchi, H. (1980) *J. Biol. Chem.* **255**, 7181-7191.
- 29- Lamparter, T., Michael, N., Caspani, O., Miyata, T., Shirai, K., & Inomata, K. (2003) *J. Biol. Chem.* **278**, 33786-33792.¶
- 30- Tate, S. S. & Meister, A. (1981) *Mol. Cell. Biochem.* **39**, 357-368.

- 31- Penrose, J. F., Austen F. K. & Lam, B. K. (1999) in: *Inflammation: basic principles and clinical correlates*. eds. Gallin J.I. & Snyderman R. (Lippincott Williams & Wilkins, Philadelphia), pp. 361-372.
- 32- Dumont, M. E., Ernst, J. F., Hampsey, D. M. & Sherman, F. (1987) *EMBO J.* **6**, 235-241.
- 33- Fairchild, C. D., Zhao, J., Zhou, J., Colson, S. E., Bryant, D.A., Glazer, A. N. (1992) *Proc. Natl. Acad. Sci. USA* **89**,7017-7021.
- 34- Schmid, R., & McDonagh, A. F. (1979) *The Porphyrins*, ed. Dolphin, D. (Academic Press, New York.) vol. VI, pp 257-292.
- 35- Drummond, G. S., & Kappas, A. (1981) *Proc. Natl. Acad. Sci. USA.* **78**, 6466-6470.
- 36- Maines, M. D. (1992) *Heme Oxygenase: Clinical Applications and Functions*, ed. Maines, M. D. (CRC Press, Boca Raton, Florida), pp 203-266.
- 37- McDonagh, A. (2001) *Nat. Struct. Biol.* **8**, 198-200.
- 38- Caignan G. A., Deshmukh, R., Wilks, A., Zeng, Y., Huang, H.W., Moennes-Loccoz, P., Bunce, R. A., Eastman, M. A. & Rivera, M. *et al.*, (2002). *J. Am.Chem. Soc.* **124**, 14879-14892.
- 39- Friedman, J., Lad, L., Li, H., Wilks, A. & Poulos, T. L. (2004) *Biochemistry* **43**, 5239-5245.
- 40- Fujii, H., Zhang, X. & Yoshida, T. (2004) *J. Am. Chem. Soc.* **126**, 4466-4467.
- 41- Rivera, M. & Zeng, Y. (2005) *J. Inorg. Biochem.* **99**, 337-354.
- 42- Wang, J., Evans, J. P., Ogura, H., La Mar, G. N. & Ortiz de Montellano, P. R. (2006) *Biochemistry* **45**, 61-73.
- 43- Kumar, S., Christophides, G. K., Cantera, R., Charles, B., Han, Y. S., Meister, S., Dimopoulos, G., Kafatos, F. C. & Barillas-Mury, C. (2003) *Proc. Natl. Acad. Sci. USA* **100**, 14139-14144.

- 44- Ha, E. M., Oh, C. T., Ryu, J. H., Bae, Y. S., Kang, S. W., Jang, I. H., Brey, P. T. & Lee, W.J. (2005) *Dev. Cell* **8**, 125-132.
- 45- Ryter, S.W. & Choi, A.M. (2005) *Antioxid. Redox. Signal.* **7**, 80-91.
- 46- Ribeiro, J. M. (1995) *Infect. Agents. Dis.* **4**, 143-152.
- 47- Holden, H. M., Rupnievski, W. R., Law, J. H. & Rayment, I. (1987) *EMBO J.* **6**,1565-1570.
- 48- Braz, G. R. C., Moreira, M. F., Masuda, H. & Oliveira, P. L. (2002) *Insect Biochem. Mol.Biol.* **32**, 361-367.

Figure Legends

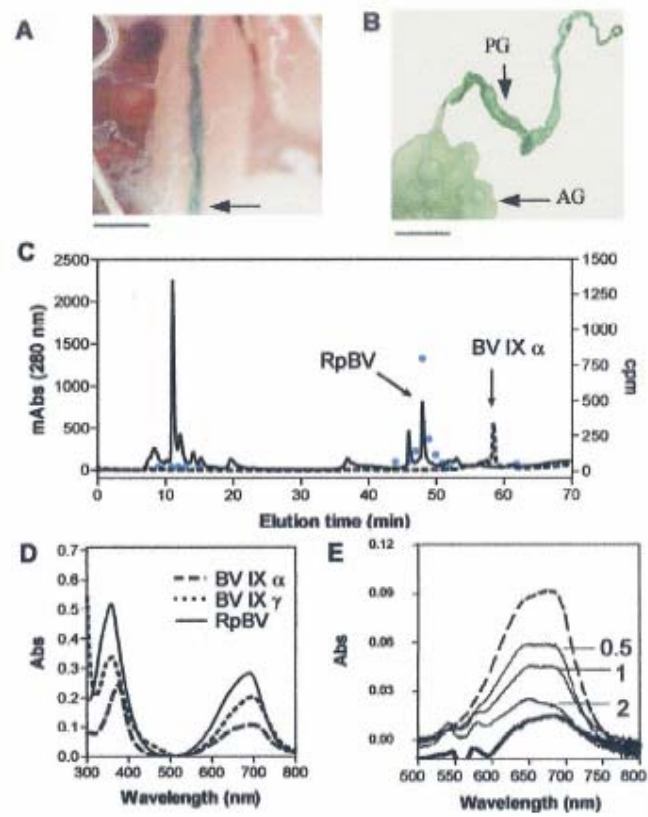
Fig. 1. *In vivo* heme degradation by *Rhodnius prolixus*. **(A)** Dorsal side of a dissected *R. prolixus* abdomen showing the green heart (arrow). **(B)** Green *R. prolixus* midgut 30 days after blood meal, when digestion is completed. AG, anterior midgut; PG, posterior midgut. **(C)** Reverse-phase HPLC profile of heart homogenate from ^{14}C -heme-injected insects (solid line). The radioactivity associated with each fraction is indicated by blue dots. The elution profile of BV IX α is shown by dashed line. **(D)** Light-absorption spectra of BV IX α (dashed line), BV IX γ (dotted line) and purified *R. prolixus* biliverdin, RpBV (solid line). **(E)** Light-absorption spectra of heart homogenates showing changes in the RpBV content after different treatments: PBS-injected control (thick solid line); insects injected with 10 nmol heme (dashed line); insects co-injected with 10 nmol heme and 0.5, 1, and 2 nmol Sn-protoporphyrin IX, as indicated (thin solid lines). Bars mean 0.5 mm in **(A)** and 0.3 cm in **(B)**.

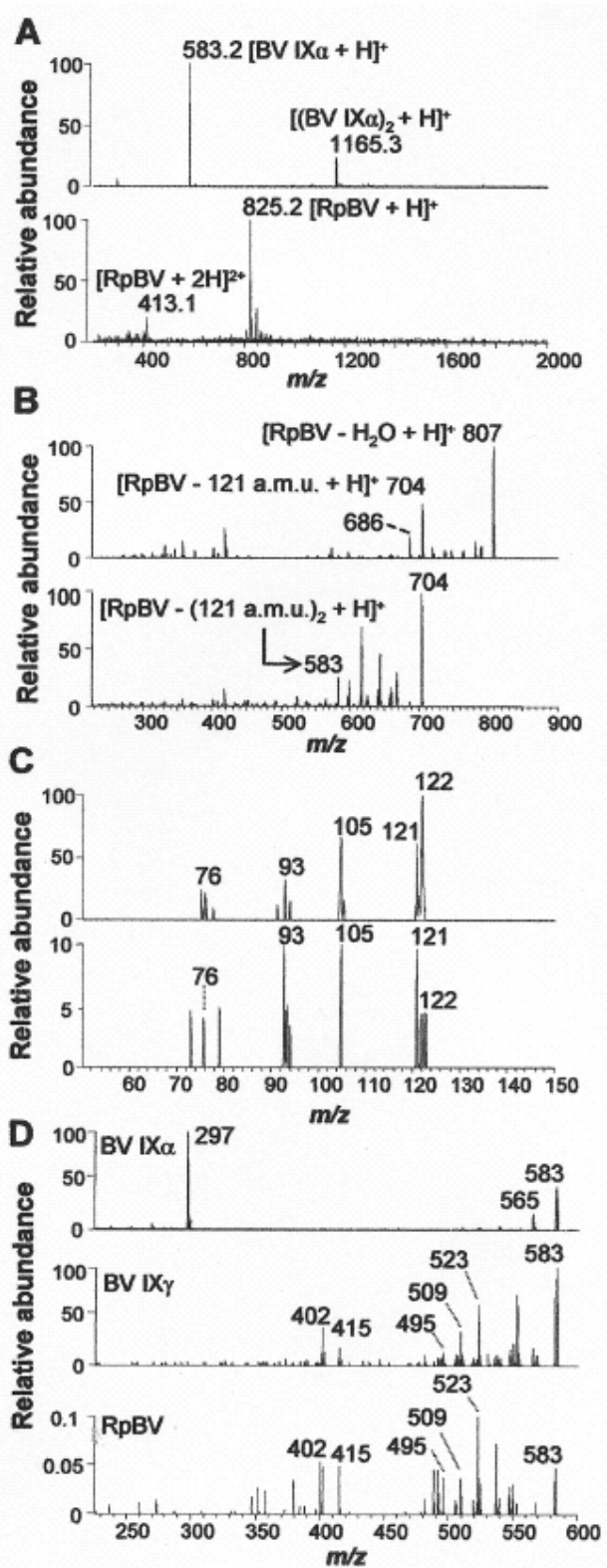
Fig. 2. ESI-MS analysis of the RpBV structure. **(A)** Mass spectra of BV IX α ($[\text{M} + \text{H}]^+$ and $[2\text{M} + \text{H}]^+$ at m/z 583.2 and 1165.3, respectively; upper spectrum), and of purified RpBV indicating a molecular mass of 824.3 Da ($[\text{M} + \text{H}]^+$ and $[\text{M} + 2\text{H}]^{2+}$ at m/z 825.2 and 413.1, respectively; lower spectrum). **(B)** Fragmentation (tandem ESI-MS) spectra of RpBV, showing daughter-ion species at m/z 704 (upper spectrum), which by further fragmentation (MS^3) gave origin to a daughter-ion species with the same molecular mass as BV IX α (m/z 583, lower spectrum). **(C)** Fragmentation patterns of authentic cysteine (upper spectrum), and the ion species at m/z 122 produced by cone fragmentation of RpBV (lower spectrum). **(D)** Identification of the RpBV isomer. Fragmentation patterns of BV IX α (upper spectrum), BV IX γ (middle spectrum) and RpBV (lower spectrum) are shown. m/z , mass to charge ratio.

Fig. 3. Characterization of the *R. prolixus* heme degradation pathway intermediates 1 and 2. **(A)** Reverse-phase HPLC analysis of insect heart homogenates. Insects were injected with PBS as a control (upper chromatogram) or co-injected with heme and SnPP IX (lower chromatogram). Peaks corresponding to RpBV, heme, and intermediates (Int) 1 and 2 are indicated by arrows. Inset: light-absorption spectra of Int 1 (solid line), Int 2 (dotted line), and heme (dashed line). **(B)** ESI-MS of Int 1 (upper spectrum) and Int 2 (lower spectrum). **(C)** tandem ESI-MS of the m/z 776 ion species generated from Int 1 (shown in Fig. 5A). Middle and lower spectra show the fragmentation profile of the daughter-ions at m/z 557 and 498, respectively. **(D)** ESI-MS/MS of the m/z 616 ion species generated from authentic heme (upper spectrum). Middle and lower spectra show the fragmentation profile of the daughter-ions at m/z 557 and 498, respectively.

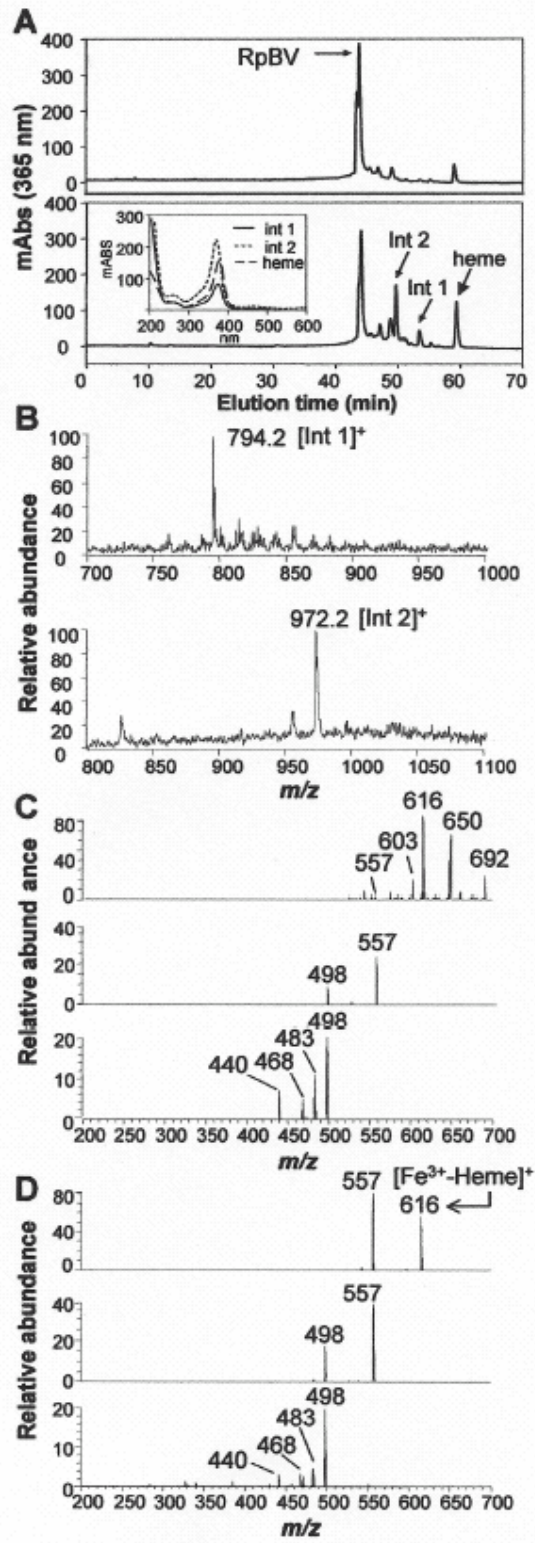
Fig. 4. The proposed heme degradation pathway in *R. prolixus*.

Paiva-Silva *et al.*, figure 1

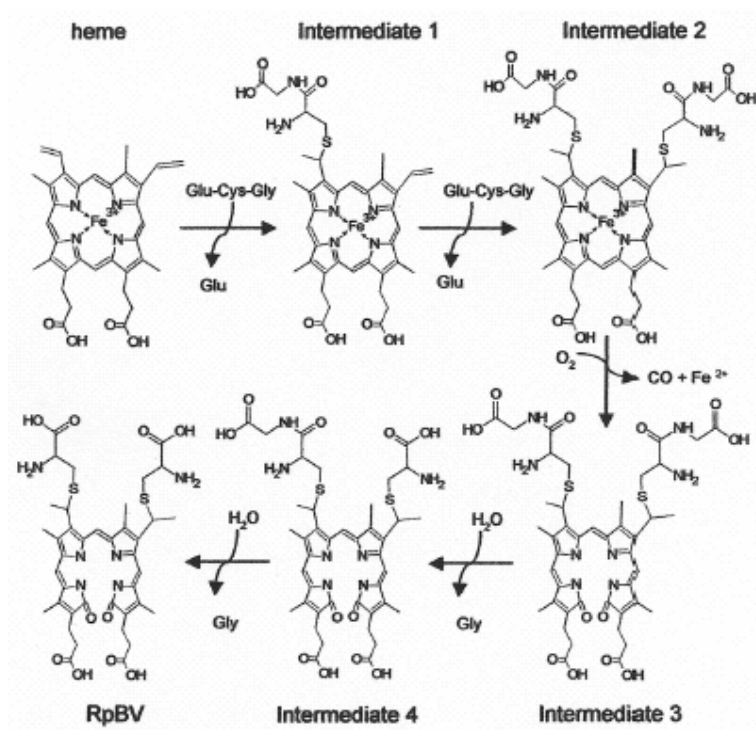




Paiva-Silva *et al.*, figure 3



Paiva-Silva *et al.*, figure 4



Supporting information

Supporting figure legends

Fig. 5. Characterization of the RpBV–cysteine bond: ESI-MS analysis of chemically modified RpBV and BV IX γ . BV IX γ (**A**) and RpBV (**B**) after *N*-acetylation of free amino groups. Methylation of carboxyl groups of BV IX γ (**C**) and RpBV (**D**). (**E**) Alkylation reaction of RpBV free SH groups. Numbers indicate the *m/z* value of each ion species. *m/z*, mass to charge ratio. (**F**) Proposed structure of RpBV.

Fig. 6. Characterization of the *R. prolixus* heme degradation pathway intermediates: addition of cysteinylglycine residues. ESI-MS fragmentation spectra of intermediate 1, monocysteinylglycine-heme (**A**) and intermediate 2, dicysteinylglycine-heme (**B**). Fragmentation of both intermediates produced a daughter-ion species at *m/z* 776 (indicated by arrows). Proposed structure for intermediate 1 (**C**) and intermediate 2 (**D**) and the assignments for the respective daughter-ions are shown. Number in parenthesis is for the respective dehydrated ion species.

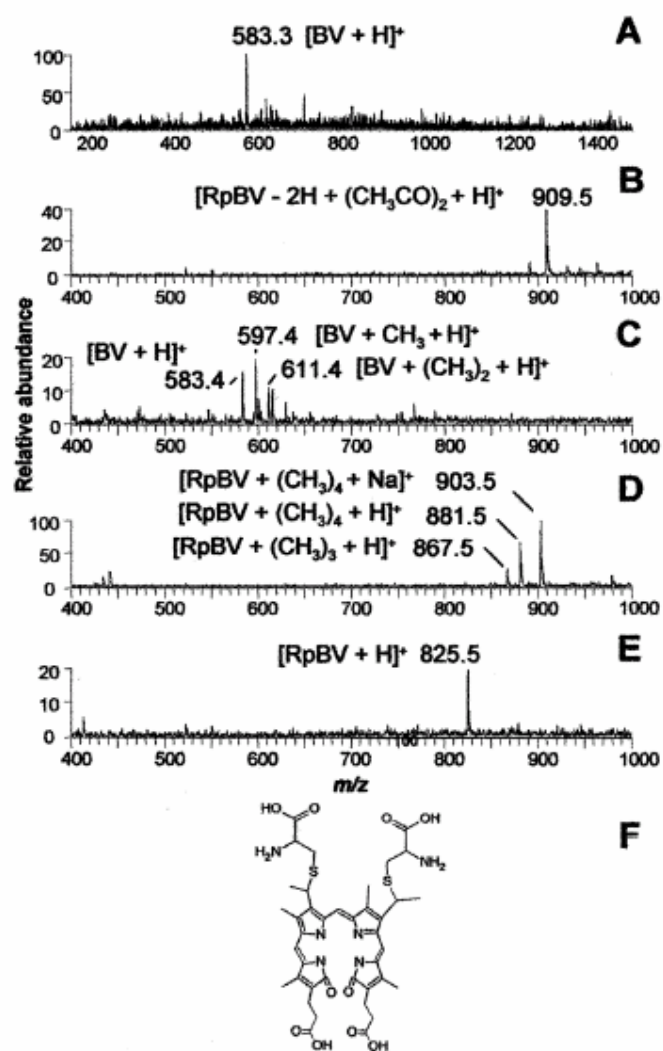
Fig. 7. Reverse-phase HPLC profile of heart homogenate from mesoheme-injected insects. The elution volume mesoBV IX α is indicated by an asterisk (*). Inset: light-absorption spectra of heme (solid line) and mesoheme (dashed line) peaks.

Fig. 8. Identification of the *R. prolixus* heme degradation pathway intermediates by LC-MS. Reverse phase nano-HPLC profile of a heart homogenate analyzed by ESI-MS. Peaks corresponding to RpBV, heme, and intermediates (Int) 1, 2, 3 and 4 are indicated by arrows (**A**). Owing to their low abundance, Int 3 (*m/z* 939.3) (**B**) and Int 4 (*m/z* 882.3) (**C**) could be

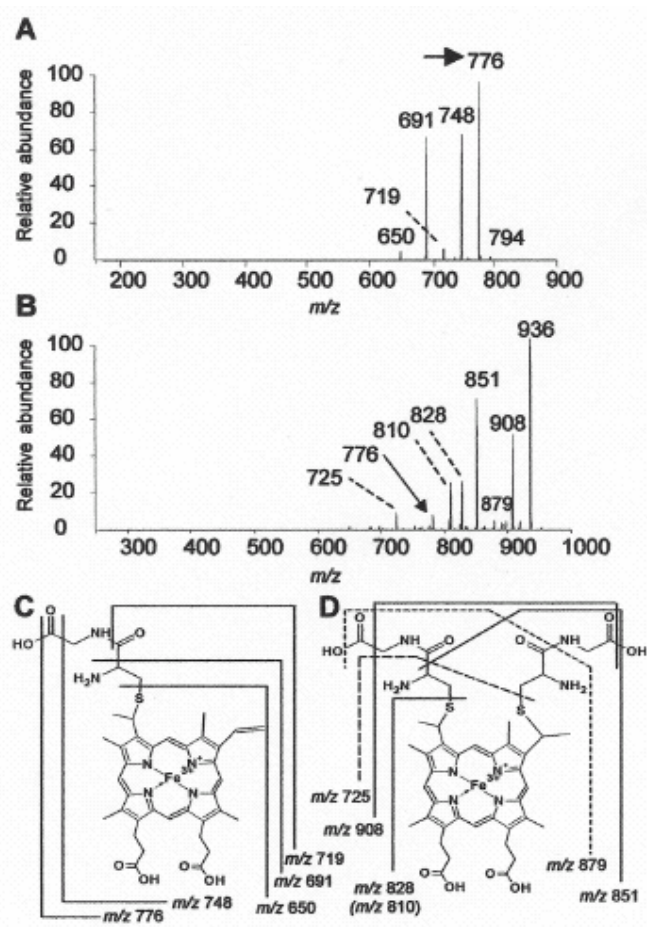
detected only by SIM analysis. The spectrum of Int 3 shows contaminating ions of RpBV (m/z 825.3) and Int 4, whereas the spectrum of Int 4 shows only a minor ion of RpBV.

Fig. 9: Characterization of the *R. prolixus* heme degradation pathway intermediates: cleavage of the porphyrin ring and trimming of the Cys-Gly residues. Tandem ESI-MS spectra of Int 3 (**A**) and Int 4 (**B**). Proposed structures of Int 3 (**C**) and Int 4 (**D**), and the respective assignments of their daughter-ions are shown. Numbers in parentheses are for the respective dehydrated ion species.

Paiva-Silva *et al.*, figure 5



Paiva-Silva *et al.*, figure 6



Paiva-Silva *et al.*, figure 7

